



# Aquaporin 1 alleviates acute kidney injury via PI3K-mediated macrophage M2 polarization

ChunMei Liu<sup>1</sup> · BoHui Li<sup>1</sup> · KaiHong Tang<sup>1</sup> · XueNing Dong<sup>1</sup> · LongGe Xue<sup>1</sup> · Guangming Su<sup>1</sup> · Yingyu Jin<sup>1</sup>

Received: 5 December 2019 / Revised: 26 February 2020 / Accepted: 7 March 2020 / Published online: 16 March 2020  
© Springer Nature Switzerland AG 2020

## Abstract

**Background** Lipopolysaccharide (LPS)-induced acute kidney injury (AKI) is associated with an abnormal immune response. Accumulating evidence has demonstrated that aquaporin 1 (AQP1) prevents kidney tissue injury in LPS-induced AKI by mediating immune response. However, the underlying mechanisms remain obscure. Macrophages as immune cells with multiple phenotypes are important mediators in tissue homeostasis and host defense. We propose that macrophage polarization is implicated in AQP1-mediated immune response.

**Methods** Herein we established sepsis-induced AKI model rats through intraperitoneal injection of LPS into Wistar rats to reveal immune mechanism of damage. We also used LPS-induced mouse RAW264.7 cells to elucidate the molecular mechanism of macrophage polarization.

**Results** Histopathology showed that renal tubular epithelial cells in the model group were swollen, inflammatory exudation was obvious and the inflammatory factors, interleukin-6 (IL-6) and tumor necrosis factor  $\alpha$  (TNF- $\alpha$ ) were increased. Western blotting showed PI3K was upregulated in the model group. Serum creatinine and urea nitrogen increased after LPS injection. Renal AQP1 mRNA is downregulated and serum AQP1 protein increased first and then decreased in LPS-induced AKI rats. M2 macrophage markers (Arg-1, CD206) were increased in repair stage. In addition, treatment of murine macrophages (RAW264.7) with AQP1 siRNA resulted in decreased PI3K activation and M2 polarization, but increased IL-6 and TNF- $\alpha$ . Moreover, inhibiting PI3K with wortmannin imitated the results of AQP1 silencing.

**Conclusions** Macrophage M2 polarization is likely the cellular mechanism underlying the anti-AKI property of AQP1, and PI3K activation is involved in the AQP1-induced M2 phenotype switch.

**Keywords** Acute kidney injury · Aquaporin 1 · Macrophage polarization · PI3K · Signaling pathway

## Introduction

Sepsis is a complex clinical condition characterized by an abnormal whole-body inflammatory response induced by a harmful response to infection [1]. It plays a critical role in the onset of acute injury of multiple organs, with the kidney being one of the most frequently involved [2]. Acute kidney injury (AKI) is the first reason for septic patients' death.

To date, the main clinical therapies for LPS-induced AKI, such as supportive care, fluid resuscitation and hemodialysis, emphasize the role of renal hemodynamic, metabolic and systemic changes. These treatments improve clinical symptoms, however, the mortality rate due to AKI remains unacceptably high at 30% [3]. There must be another pathological mechanism in the process of AKI except for hemodynamic change. An increasing number of studies have indicated that renal inflammation is one of the main pathological changes observed in AKI [4]. Therefore, controlling abnormal immune responses in the kidney may prevent AKI and improve the clinical prognosis of sepsis.

Overwhelming evidence suggests that aquaporins are not only involved in the molecular transport, but are also associated with several pathological conditions, including malignancies, glaucoma and inflammatory diseases [5–7]. Many studies have found that downregulation of aquaporin

Responsible Editor: John Di Battista.

✉ Yingyu Jin  
jyyharbin@163.com

<sup>1</sup> Department of Laboratory Diagnosis, The First Affiliated Hospital of Harbin Medical University, 23 Youzheng Street, Nangang District, Harbin 150001, Heilongjiang, People's Republic of China

expression is a major pathological mechanism of inflammatory organ injury, through weakening the inhibition of overactivated inflammation [8, 9]. At present, 13 mammalian aquaporins have been identified, of which AQP1 is the principal subtype that plays a major role in the regulation of inflammation [10]. Moreover, AQP1 is highly expressed in proximal tubular epithelial cells [10]. It has been reported that AQP1 overexpression in hepatocytes improves LPS-induced cholestasis [11]. Furthermore, a previous study has demonstrated that AQP1 overexpression inhibited the aristolochic acid I-induced epithelial–mesenchymal transition of HK-2 cells, suggesting that AQP1 may be a target for aristolochic acid nephropathy clinical therapy [12]. Another study that supports the protective effect of AQP1 on AKI found that AQP1 inhibits M2 polarization under normal conditions and promotes M2 polarization after LPS stimulation [13] to regulate the inflammatory response. Our previous studies have also found that AQP1 expression was elevated in the early stage of AKI [14]. Furthermore, overexpression of the *AQP1* gene reduced the release of inflammation factors and alleviated cell apoptosis in LPS-induced HK-2 cells [15]. Whether AQP1 alleviates inflammation by promoting M2 polarization remains largely unknown. The protective effect of AQP1 on LPS-induced RAW264.7 cells remains to be elucidated.

Organ hypoperfusion caused by hemodynamic disturbance has long been considered as a major pathological mechanism of acute renal injury caused by sepsis [16]. However, with the advances in research on the inflammation mechanism of renal injury, it appears that AKI is an inflammatory disease [1]. Cell damage and inflammation are the two critical pathological mechanisms of AKI. Inflammatory cell infiltration and renal tubular epithelial cell swelling as well as degeneration and partial necrosis have been observed in rat renal tissues exposed to LPS. Typically, inflammatory cell infiltration is primarily ascribed to lymphocytes and neutrophils. However, other cell types have also been found to play an important role in the initiation and progression of inflammation, including macrophages [17]. Macrophage polarization is a unique form of inflammatory cell activation that is dependent on activation of specific intracellular signaling pathways. Damage and repair stimuli can polarize resting macrophages into proinflammatory M1 and pro-repair M2 cells, respectively [18]. Recently, it has been reported that macrophage polarization is involved in LPS-induced inflammation [19, 20] and that the macrophage polarization state determines the inflammation outcome, suggesting a potential role for macrophage polarization in AKI induced by sepsis.

Located in the renal tissue, macrophages constitute a protective barrier against pathogen infection. In addition, macrophage activation is a crucial and initial stage in the development of AKI caused by sepsis [21, 22]. The different

polarization subtypes of macrophages determine the inflammation outcome. However, phenotypic transformation of macrophages requires precise regulation of complex signaling pathways. PI3K is considered to be a classical signaling pathway for promoting autophagy and regulating inflammation; extracellular signaling molecules can active PI3K to induce the activation of downstream molecules, ultimately leading to pathophysiological changes [23]. Recent studies have shown that PI3K activation in macrophages promoted macrophage M2 polarization, alleviated tissue damage and promoted repair. Additionally, a PI3K inhibitor decreased peritoneal macrophage M2 polarization induced by IL-4/IL-13 [13, 24]. Herein we used PI3K inhibitors to confirm the effect of PI3K on macrophage M2 polarization in LPS-induced RAW264.7 cells.

Previous studies have shown that AQP1 can alleviate LPS-induced cell injury [15], however, the cellular and molecular mechanisms remain unknown, which prevents the application of targeted therapy for AKI. We therefore conducted the present study to explore the potential role of AQP1 in macrophage polarization in a rat model of AKI. We also investigated the molecular and signaling mechanisms underlying the AQP1 effect.

## Materials and methods

### Animals and establishment of AKI model

Nine-week-old male Wistar rats (180–200 g) were purchased from the Laboratory Animal Center of Harbin Medical University and were kept under standard animal room conditions of  $22 \pm 1$  °C and of  $55 \pm 5\%$  humidity. The rats had free access to water and food.

The study protocol was approved by the Animal Care and Use Committee of Harbin Medical University and the experimental procedures were in accordance with the recommendations of the Guide for the Care and Use of Laboratory Animals, published by the US National Institutes of Health (NIH Publication no. 85–23. Revised 196).

The rats were randomly divided into five groups (three animals in each group): normal saline group (NS), 12 h of LPS treatment group (12 h), 24 h of LPS treatment group (24 h), 48 h of LPS treatment group (48 h) and 72 h of LPS treatment group (72 h).

To establish the endotoxemic AKI model, the rats were injected intraperitoneally with  $10 \text{ mg}\cdot\text{kg}^{-1}$  body weight of LPS (Sigma–Aldrich, St. Louis, MO, USA; dissolved in 600  $\mu\text{L}$  of pyrogen-free saline). The control group received 600  $\mu\text{L}$  of pyrogen-free saline. The rats were euthanized with 10% chloral hydrate and killed. Blood was collected in heparinized tubes and bilateral kidneys were removed, with one kept at  $-80$  °C [for enzyme-linked immunosorbent

assay (ELISA), qPCR and western blot analysis] and the other fixed in 4% paraformaldehyde (for histopathology and immunofluorescence staining).

### Biochemical analysis of renal function

To assess renal function, blood samples were collected and centrifuged at 2000 g for 10 min at room temperature and the supernatant was placed in sterile tubes for storage at  $-80^{\circ}\text{C}$ . Serum urea nitrogen (BUN) and creatinine were measured with an automatic biochemical analyzer (Vitros<sup>®</sup> V5600, Ortho Clinical Diagnostics, Raritan, NJ, USA). A 1.5-fold increase in creatinine compared with the control group represents a successful establishment of the AKI model.

### Kidney tissues histopathology

Kidney tissues were removed from the rats and fixed with 4% paraformaldehyde, followed by embedding in Optimum Cutting Temperature (OCT) compound (SAKURA, San Francisco, CA, USA) for evaluation of kidney tubular cell damage and inflammatory exudation. Renal sections of 4  $\mu\text{m}$  thickness were stained with hematoxylin and eosin (H&E) using standard procedures.

### RNA extraction and real-time qPCR

Total RNA from kidney tissues and cells was extracted using TRIzol reagent (Invitrogen, Carlsbad, CA, USA), according to the manufacturer's protocol. The concentration and purity of extracted RNA were determined with an ultramicro spectrophotometer K5600 (KAIAO, Beijing, China). The RNA was incubated in a metal bath (HB120-s) at  $65^{\circ}\text{C}$  for 5 min, and then a Script cDNA synthesis kit (Bio-Rad, Hercules, CA, USA) was used for the reverse transcription of the extracted RNA. Changes in target genes' mRNA levels were measured by relative real-time qPCR with a Bio-Rad CFX96 real-time qPCR Detection System.

The qPCR reaction volume was 20  $\mu\text{L}$  and included cDNA, dNTPs, primers, SYBR Green Supermix (Bio-Rad) and nuclease-free water. Amplifications were carried out with the following cycling conditions: 40 cycles of denaturation at  $95^{\circ}\text{C}$  for 5 s, annealing at  $55^{\circ}\text{C}$  for 10 s and elongation at  $72^{\circ}\text{C}$  for 15 s. The expression of *AQP1* mRNA was normalized to the mRNA level of *GAPDH*. Results were calculated using the  $2^{-\Delta\Delta\text{Ct}}$  method and each experiment was performed in triplicate. The primer sequences used for the experiment are as follows: *AQP1*: 5'-ACCTGCTGGCCATTGACTAC-3' and 5'-CCAGGGCACTCCCAATGAAT-3'; *Actin*: 5'-CGCGAGTACAACCTTCTTGC-3' and 5'-CCAGGGCAC TCCCAATGAAT-3'.

## Cell culture, transfections and treatment

### Cell culture

The mouse macrophage cell line RAW264.7 was obtained from American Type Culture Collection and maintained in Dulbecco's modified eagle's medium (DMEM) supplemented with 10% fetal bovine serum (FBS; Gibco; Thermo Fisher scientific, Inc., Waltham, MA, USA) and 1% penicillin/streptomycin. The cells were cultured at  $37^{\circ}\text{C}$  with 5%  $\text{CO}_2$  and 95% air.

### Cell transfection

RAW264.7 cells were transiently transfected with 100 nM si-AQP1 for 4 h (Invitrogen, Thermo Fisher Scientific, Waltham, USA) using Lipofectamine 2000 reagent (Invitrogen) according to the manufacturer's instructions. After 4 h, the medium was replaced with fresh medium, and after 24 h, the cells were harvested for detection of transfection efficiency using qPCR (Table 1).

### Cell treatment

The cell experiments were divided into five groups: control group, transfection group, LPS treatment group, transfection + LPS treatment group, and wortmannin (PI3K inhibitors) pretreated + LPS treatment group. After 24 h of transfection, cells were stimulated with  $0.1 \mu\text{g}\cdot\text{mL}^{-1}$  LPS (Sigma-Aldrich) for 6 h, followed by  $0.05 \mu\text{g}\cdot\text{mL}^{-1}$  LPS for 18 h, or pretreated with 100 nM wortmannin for 1 h and subsequently treated with LPS (the concentration and time as described above) for 24 h. Then, the medium was replaced with fresh medium. Pseudopodia formation was observed under an inverted microscope every day. Timing started after removing the LPS; each group of cells was harvested and the supernatant was collected at 4, 24 and 48 h. Harvested cells and supernatants were stored at  $-80^{\circ}\text{C}$  for protein/RNA extraction and ELISA analysis.

**Table 1** Transfection efficiency of *AQP1*

	Control	NC	No1	No2	No3
<i>Actin</i>	21.25	21.76	20.80	20.22	20.46
	20.67	20.95	20.97	19.77	21.19
	20.98	21.34	21.23	20.36	21.01
<i>AQP1</i>	26.10	27.01	29.69	32.00	28.92
	26.61	27.56	30.58	31.14	28.58
	26.94	27.86	31.21	31.53	28.39
Average $2^{-\Delta\Delta\text{Ct}}$	1.00	0.69	0.07	0.02	0.27

## Cellular immunofluorescence

Immunofluorescence staining was performed to determine the cellular distribution of CD206 and NF- $\kappa$ B in RAW264.7 cells. Briefly, RAW264.7 cells were seeded in 24-well plates containing 1-cm sterile glass coverslips. Cell transfection and treatment was performed as described above. After treatment, cells were fixed with 3.2% paraformaldehyde for 15 min and permeabilized with 0.1% TritonX-100 in phosphate-buffered saline (PBS) for 1 h at room temperature. Non-specific staining was prevented by incubation with 1% bovine serum albumin. Cells were washed with PBS five times and then incubated with anti-CD206 (Abcam, London, UK,; 1:500) or anti-NF- $\kappa$ B antibody (Abcam; 1:250) at 4 °C overnight. After rinsing with PBS three times, the cells were incubated with fluorescent dye-conjugated secondary antibodies CD206 or NF- $\kappa$ B (Abcam 1:500) in the dark for 1 h. The cells were imaged using an Olympus fluorescence microscope (Olympus Fluoview1000, Tokyo, Japan).

## Western blotting

Following treatment, kidney tissue samples and RAW264.7 cells were lysed in complete RIPA lysis buffer (Sigma-Aldrich) with protease inhibitor cocktail (Sigma-Aldrich) to extract proteins. The protein concentration was quantified using a BCA protein Assay kit (Bio-Rad). Equal amounts of protein lysates (30  $\mu$ g) were separated by 10% SDS-polyacrylamide gel electrophoresis and transferred to polyvinylidene fluoride membranes (Millipore, MA, USA) with a wet transfer apparatus. The membranes were blocked with 5% skim milk diluted with Tris-buffered saline with Tween 20 (TBST) at room temperature for 2 h. After blocking, membranes were incubated with primary antibodies against PI3K (Abcam; 1:1000) overnight at 4 °C. The membranes were washed and incubated with an anti-rabbit IgG conjugated to horseradish peroxidase for 2 h at 4 °C. The density of the bands was determined using a 5200 automatic chemiluminescence Image Analysis System (TianNeng, Shanghai). Values were normalized to the densitometric values of GAPDH (Abcam; 1:1000).

## Enzyme-linked immunosorbent assay

Kidney tissues, rat blood, RAW264.7 cells and the supernatants of RAW264.7 cells were analyzed. The concentrations of IL-6, TNF- $\alpha$ , AQP1, inducible nitric oxide synthase (iNOS; M1 marker) and Arog-1 (M2 marker) were measured using a sandwich ELISA kit (Shanghai Enzyme Linked Biology CO., Ltd. Shanghai, China) according to the manufacturer's instructions. Absorbance was detected at 450 nm by an automated ELISA reader (MULTISKAN FC, Thermo,

MA, USA). Concentrations in the samples were calculated using a standard curve and results are expressed in ng/mL.

## Statistical analysis

Values are expressed as mean  $\pm$  SEM. GraphPad Prism 5.0 software was used to process the data. The significance of differences was tested by Student's *t* test for two-group comparisons or one-way analysis of variance (ANOVA) for comparisons among multiple groups. \**p* < 0.05 was considered statistically significant.

## Results

### Establishment of AKI model by LPS injection

To examine the whole pathological process of kidney tissue from injury to repair, we induced AKI in rats by intraperitoneal injection of LPS. The concentration of LPS and injection volume were explored in a preliminary experiment (data not shown). The AKI model was established successfully by intraperitoneal injection of 600  $\mu$ L of 10 mg·kg<sup>-1</sup> LPS. The levels of serum creatinine and urea nitrogen were measured by an automatic biochemical analyzer. Serum creatinine was twofold higher in the model group than in the control group, indicating that the model was successfully established (Table 2). Pathological sections of the kidney were stained with H&E. The kidney histopathological images indicated that the renal tubular epithelial cells were swollen, the histological structure was disordered and inflammatory cell infiltration was significantly increased in the model group, and the kidney tissue in the control group was not histologically altered (Fig. 1a–e). Furthermore, ELISA showed increased release of the inflammatory factors, IL-6, TNF- $\alpha$  and iNOS, in kidney tissue and serum at 12 h after LPS treatment (Fig. 2a–c).

**Table 2** Serum creatinine and urea nitrogen in rats

	Serum creatinine	Urea nitrogen
Control	37.03 $\pm$ 4.27	4.71 $\pm$ 0.26
LPS 12 h	84.03 $\pm$ 6.87 <sup>a</sup>	16.42 $\pm$ 2.82 <sup>a</sup>
LPS 24 h	205.9 $\pm$ 4.26 <sup>b</sup>	41.44 $\pm$ 3.13 <sup>b</sup>
LPS 48 h	66.53 $\pm$ 1.42 <sup>c</sup>	17.03 $\pm$ 0.50 <sup>c</sup>
LPS 72 h	52.47 $\pm$ 1.96	10.88 $\pm$ 0.95 <sup>d</sup>

Data are presented as mean  $\pm$  SEM

Serum creatinine are expressed as  $\mu$ mol/L and urea nitrogen are expressed as mmol/L

<sup>a</sup>*p* < 0.05 vs. control group

<sup>b</sup>*p* < 0.05 vs. LPS 12 h

<sup>c</sup>*p* < 0.05 vs. LPS 24 h

<sup>d</sup>*p* < 0.05 vs. LPS 48 h

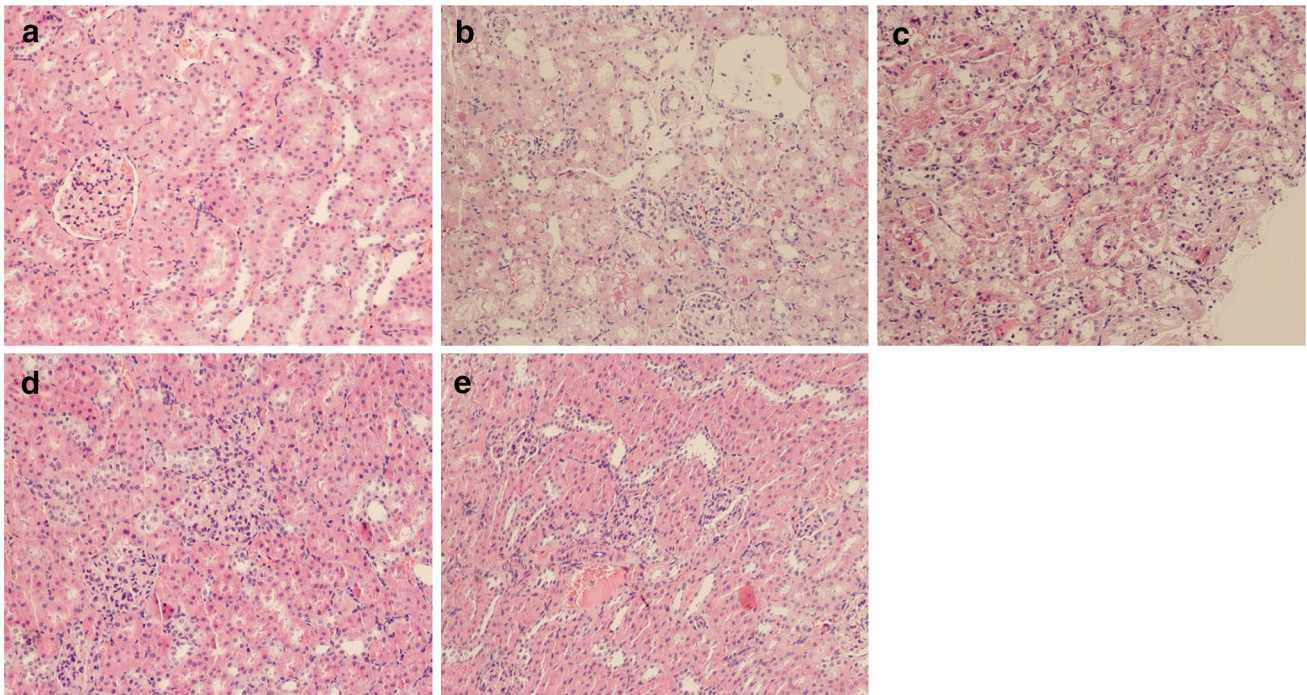


**Fig. 1** Injury pathology of the renal tissue of rats with LPS-induced AKI. Photomicrographs of H&E stained kidney sections (200 $\times$ ). **a** control group: the structure of renal tubular lumen was well defined, cells were arranged neatly, and the basement membrane was intact; no inflammatory infiltration was observed in the interstitium. **b** LPS 12 h: the renal tubular lumen was slightly dilated, with vascular congestion, and some inflammatory cell infiltration in the perivascular tissue. **c** LPS 24 h: the renal tubular lumen was obviously dilated

and the renal tubular epithelial cells degenerated, but necrosis was not observed; massive inflammatory infiltration was observed in the interstitium. **d** LPS 48 h: compared with the LPS 24 h group, epithelial cell necrosis and exfoliation to lumen were observed and inflammatory cell infiltration was further aggravated. **e** LPS 72 h: compared with the LPS 48 h, renal tissue injury and inflammatory exudation were increased

### Macrophages switch from M1 to M2 phenotype during tissue damage repair

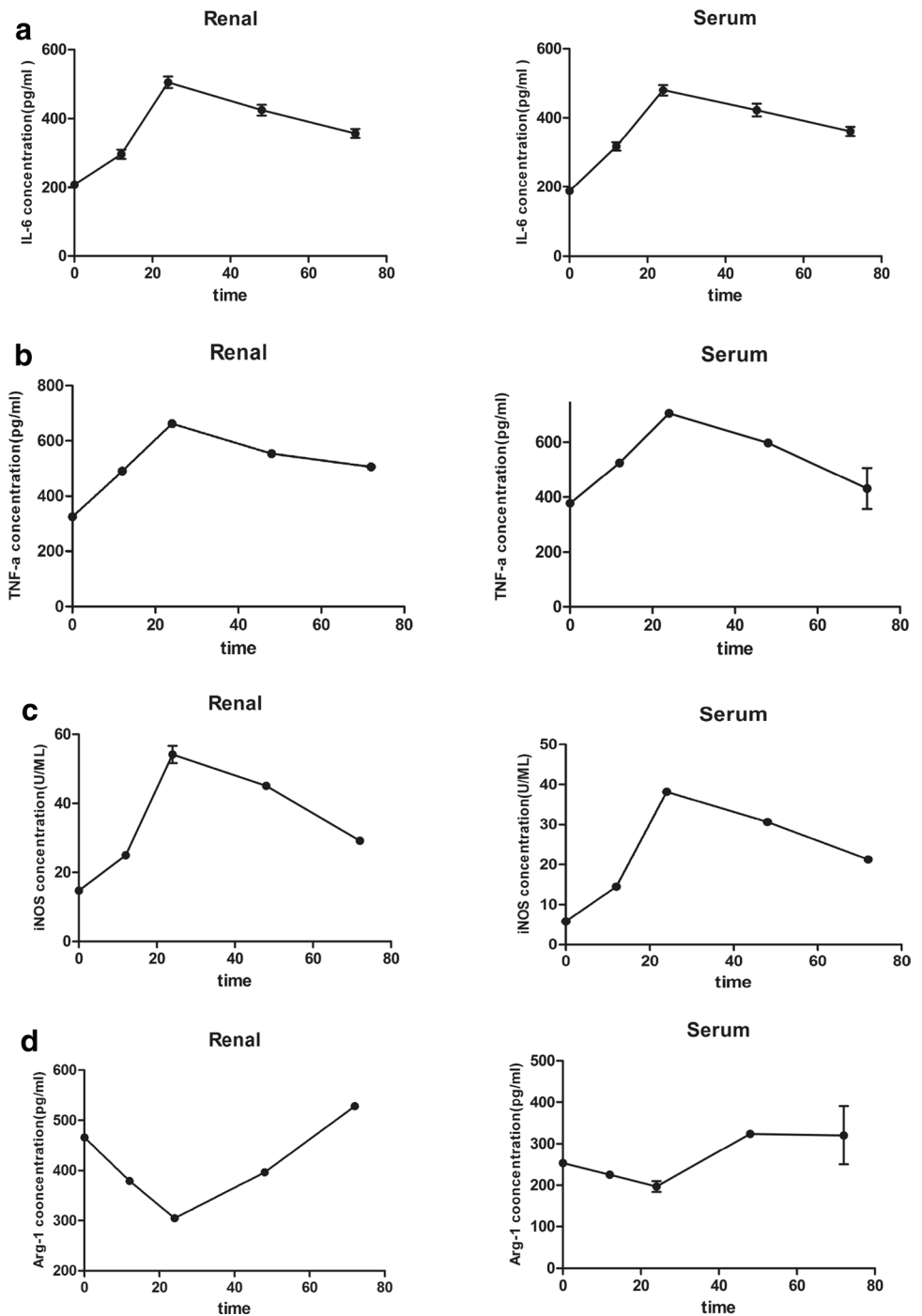
The tissue damage repair process must be accompanied by inflammation. We asked what mechanisms regulate early tissue damage and late repair. Many studies suggest that the plasticity of macrophage polarization plays a key role in the different stages of inflammation [17]. In recent years, it was found that M2 macrophages secrete growth factor TGF- $\beta$  and anti-inflammatory factor IL-10 to promote tissue repair and regeneration. On the contrary, M1 macrophages tend to express the proinflammatory cytokines to aggravate inflammation damage in tissues [18]. We hypothesized that M1/M2 polarization of macrophages regulates the balance between proinflammatory and anti-inflammatory factors, which determine the inflammation outcome. To verify this hypothesis, we examined the levels of M1/M2 macrophage polarization markers by ELISA at 0, 12, 24, 48 and 72 h after LPS stimulation. The results of ELISA (Fig. 2a–c) showed that the IL-6, TNF- $\alpha$  and iNOS (M1 markers) quickly increased in the damage stage and then gradually decline in the repair stage. In contrast, the level of Arg-1 in the renal tissue and the serum was slightly increased in the early stage,

but then significantly increased at 48 h, and remained high at 72 h (Fig. 2d). The results of kidney tissue morphology and the levels of serum creatinine and urea nitrogen collectively suggest that the kidney began to damage at 12 h, was the most serious at 24 h, and then began to repair at 48 h after treatment with LPS. Taken together, these results indicated that there is a polarization trend from M1 to M2 during the process of tissue damage to repair.

### Renal *AQP1* mRNA is downregulated and serum *AQP1* protein increased first and then decreased in LPS-induced AKI rats

In our previous study, we showed that *AQP1* in the blood and urine began to increase in the early stage of LPS-induced AKI in rats [14]. To clarify the mechanism of *AQP1* upregulation, we performed ELISA to test *AQP1* levels (Fig. 3a) in the blood and kidney tissues of rats and real-time qPCR to measure the expression of *AQP1* mRNA in kidney tissues of rats (Fig. 3b). A significant decrease in renal *AQP1* mRNA was observed in the LPS group compared with the control group. Interestingly, the ELISA revealed that *AQP1* protein in the serum and kidney tissue increased at 12 and 24 h, but

**Fig. 2** Inflammation and macrophage polarization in LPS-induced Wistar rats at different stages. **a–d** Expression profile of IL-6 (M1 marker and inflammatory factors), TNF- $\alpha$  (M1 marker and inflammatory factors), iNOS (M1 marker and inflammatory factors) and Arg-1 (M2 marker) in renal tissue and serum assessed by ELISA (Wistar rats were intraperitoneally injected with 10 mg/kg LPS; 12, 24, 48, 72 h after the injection were the time points of observation). The data are presented as the mean  $\pm$  SEM.  $p < 0.05$  compared with the previous time point



decreased at 48 and 72 h. Namely, the renal *AQP1* mRNA expression decreased, whereas the protein level increased at the early phase of AKI, suggesting that AQP1 protein may play a protective role in AKI.

### PI3K is involved in LPS-induced AKI

A growing number of studies have shown that the PI3K signaling pathway not only regulates cell autophagy, but it is also

involved in the activation and outcome of the inflammatory response [23]. As an important inflammatory signaling pathway, it regulates the balance between proinflammatory and anti-inflammatory factors. To explore the role of PI3K in LPS-induced AKI in rats, we measured the protein expression levels of PI3K in rat renal tissue after treatment with LPS by western blotting. As depicted in Fig. 4a–d, PI3K was significantly upregulated by LPS, indicating that PI3K may play a role in LPS-induced AKI.

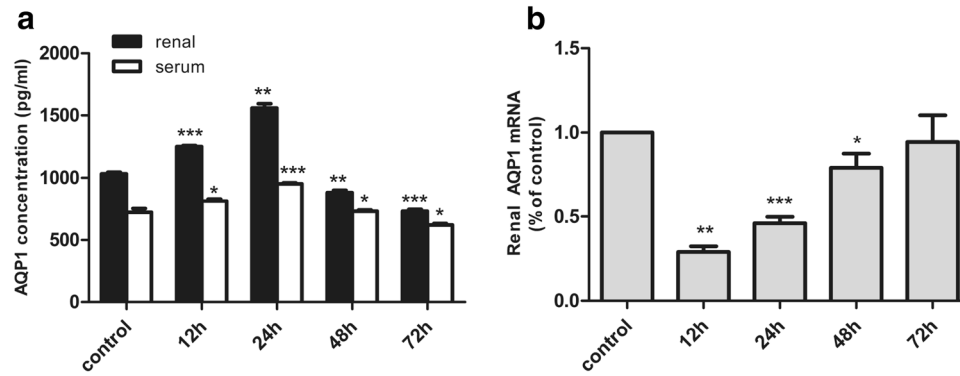


**Fig. 3** Effect of LPS on the expression of *AQP1* protein in the renal tissue of rats and *AQP1* mRNA in the serum and renal tissue. **a** *AQP1* protein levels in the renal tissue and serum were examined by ELISA. The data are presented as the mean  $\pm$  SEM. **b** Expression of

*AQP1* mRNA in the renal tissue was determined by qPCR. The data are presented relative to the control group. Each group was compared with the control group. \* $p < 0.05$ , \*\* $p < 0.01$ , \*\*\* $p < 0.001$

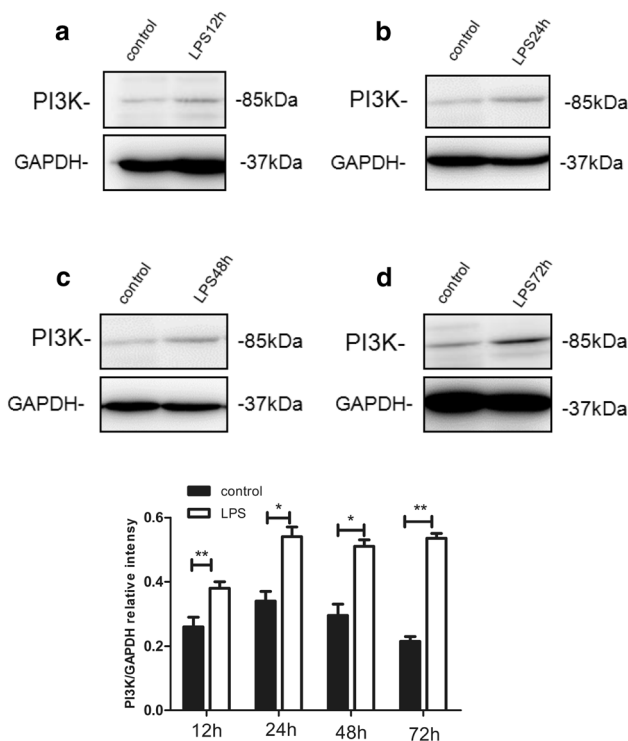


**Fig. 4** Activation of the PI3K signaling pathway in rat renal tissue treated with LPS. **a–d** Expression of PI3K protein in the renal tissue of LPS-induced Wistar rats was examined by western blotting. **a** After 12 h, **b** after 24 h, **c** after 48 h and **d** after 72 h after LPS treatment. Wistar rats were intraperitoneally injected with 10 mg/kg LPS

### Silencing *AQP1* aggravates inflammation in LPS-induced RAW264.7 cells

In the animal experiments, we established an AKI model by intraperitoneal injection of LPS and found that *AQP1* mRNA expression was robustly downregulated in the LPS group, however, the *AQP1* protein expression in the kidney

was substantially enhanced by LPS in the early stages. Thus, we speculated that *AQP1* increased in response to damage and may prevent progressive damage. To evaluate whether *AQP1* is involved in the inhibition of inflammatory activation, si-*AQP1* was transfected into RAW264.7 cells, which were then treated with  $0.1 \mu\text{g}\cdot\text{mL}^{-1}$  LPS. Interestingly, our ELISA results revealed that *AQP1* silencing significantly increased the levels of IL-6, TNF- $\alpha$  and iNOS (Fig. 5a–c). Moreover, NF- $\kappa$ B nucleus translocation increased by this treatment (Fig. 5d). These results suggest that silencing *AQP1* aggravated the inflammation in RAW264.7 cells, which is consistent with the previous animal experimental results.

### Silencing *AQP1* suppresses M2 polarization in LPS-induced RAW264.7 cells

Our in vivo results showed that the expression level of an M2 macrophage marker increased during the AKI from damage to repair and that *AQP1* protein increased in AKI rats. We also found that *AQP1* downregulated cytokine levels in RAW264.7 cells exposed to LPS. The goal of this study was to investigate whether *AQP1* protects RAW264.7 cells from inflammatory injury by enhancing M2 polarization. We treated cells with LPS to establish a cell damage model and then compared the changes in M2 macrophage markers between the control group and si-*AQP1* group. The ELISA of Arg-1 indicated that the M2 phenotype was suppressed by silencing *AQP1* gene (Fig. 6b). We also examined the M2 macrophage-specific marker, CD206, by immunofluorescence staining. The results further showed that *AQP1* silencing obviously suppressed CD206 migration to the cytoplasm (Fig. 6a). These results showed that silencing *AQP1* inhibited the M2 subtype conversion.

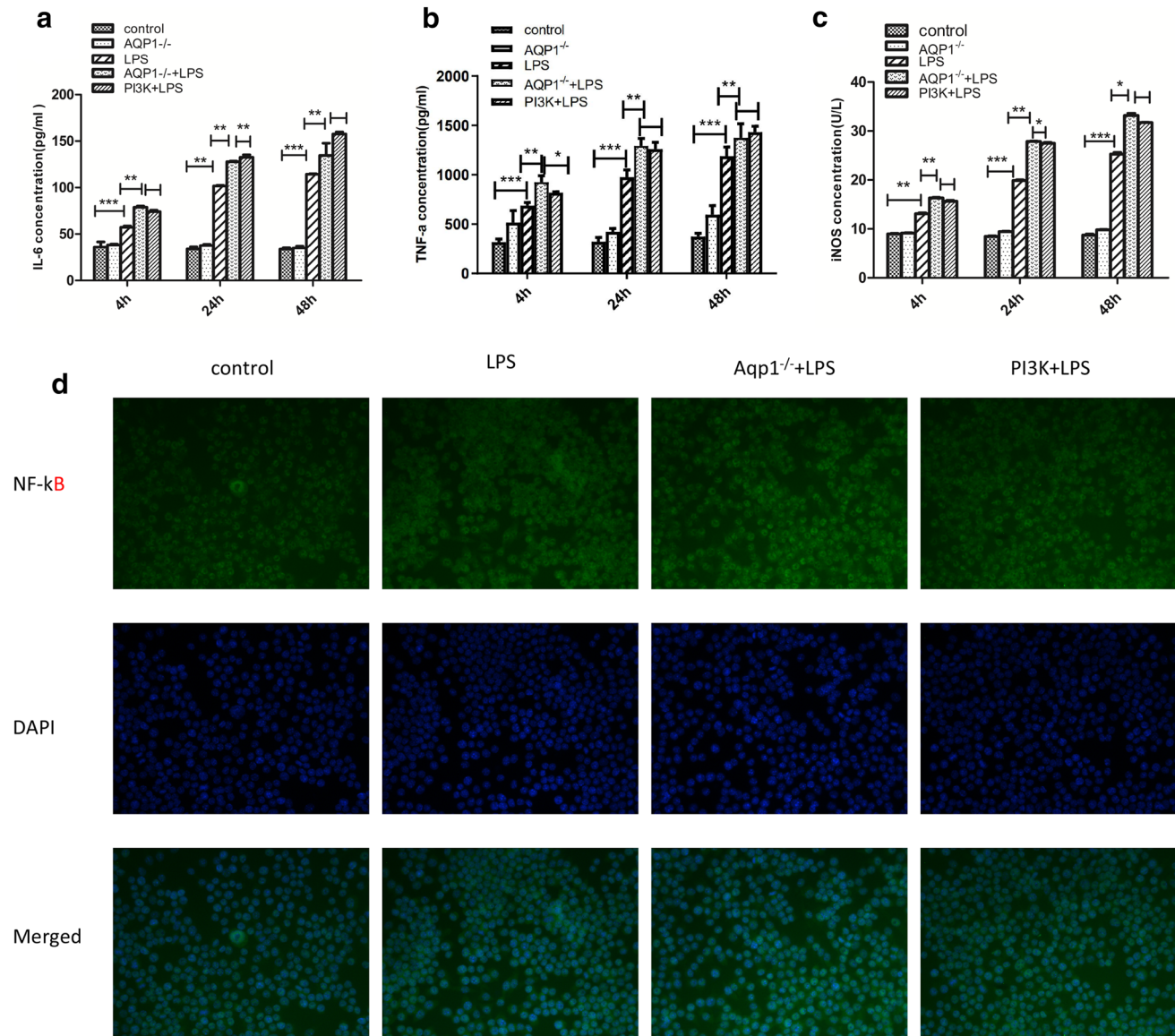


**Fig. 5** AQP1 alleviates inflammation in LPS-induced RAW264.7 cells. **a–c** Expression levels of IL-6, TNF- $\alpha$  and iNOS in RAW264.7 cells supernatants as determined by ELISA. \* $p < 0.05$ , \*\* $p < 0.01$ , \*\*\* $p < 0.001$ . Error bars represent SEM. **d** Location of NF- $\kappa$ B protein (activated NF- $\kappa$ B located in the nucleus) was detected at 24 h by immunofluorescence staining (400 $\times$ ). AQP1<sup>-/-</sup> group:

AQP1 gene silencing group with 100 nM si-AQP1 for 4 h; LPS group: RAW264.7 cells were treated with 0.1  $\mu$ g/mL LPS for 24 h; PI3K+LPS group: cells pretreated with 100 nM PI3K inhibitor (wortmannin) for 1 h and subsequently treated with 0.1  $\mu$ g/mL LPS for 24 h. 4 h, 24 h and 48 h: time after the withdrawal of LPS

### Silencing AQP1 downregulates PI3K expression in RAW264.7 cells

The in vivo experiments showed that AQP1 protein was upregulated in AKI rats' renal tissue compared with the control group. Furthermore, western blot analysis of PI3K demonstrated that its expression levels were remarkably elevated

after LPS treatment of rats. To elucidate the relationship between AQP1 and PI3K, we performed in vitro experiments on RAW264.7 cells. We examined PI3K levels after LPS administration by western blotting. The results revealed decreased PI3K protein levels following si-AQP1 transfection (Fig. 7a–c). These results indicated that silencing the AQP1 gene suppressed the PI3K activation.



**Fig. 6** Effect of AQP1 and PI3K on M2 polarization. **a** Location of CD206 protein( activated CD206 protein located in the cytoplasm) was detected at 48 h by immunofluorescence staining (400×). **b** Arg-1 levels in RAW264.7 cells as determined by ELISA. \* $p < 0.05$ , \*\* $p < 0.01$ , \*\*\* $p < 0.001$ . Error bars represent SEM. AQP1<sup>-/-</sup> group: *AQP1* gene silencing group with 100 nM si-AQP1 for 4 h; LPS group: RAW264.7 cells treated with 0.1 μg/mL LPS for 24 h; PI3K + LPS group: cells pretreated with 100 nM PI3K inhibitor (wortmannin) for 1 h and subsequently treated with 0.1 μg/mL LPS for 24 h. 4 h, 24 h and 48 h: time after the withdrawal of LPS

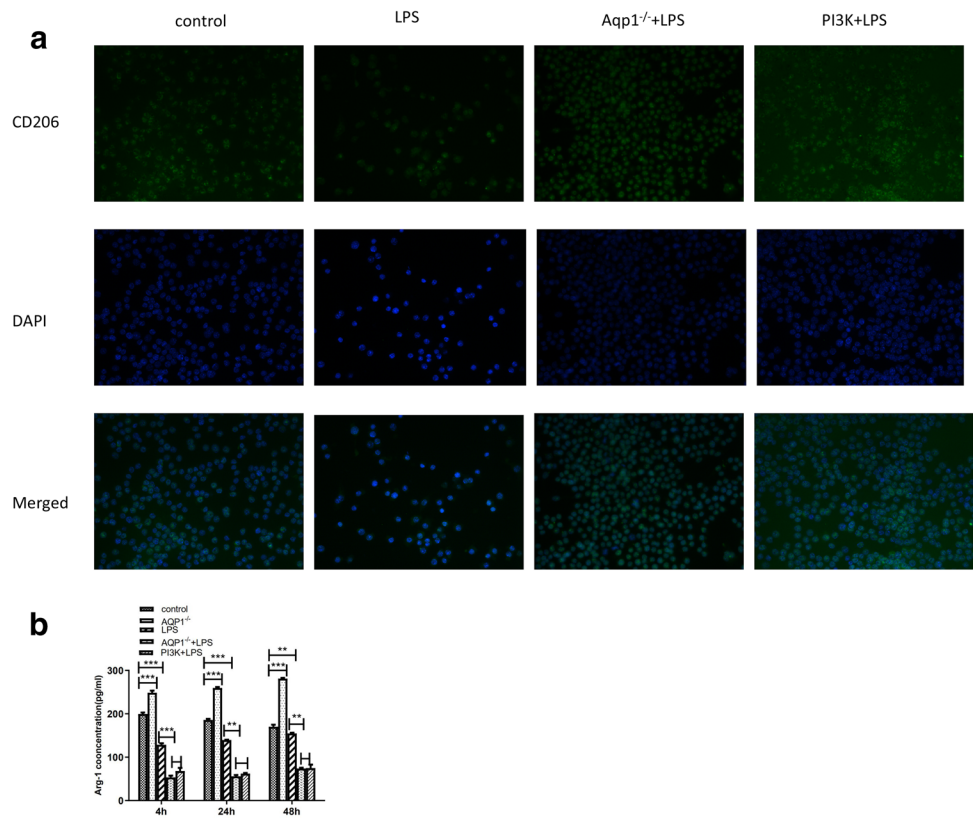
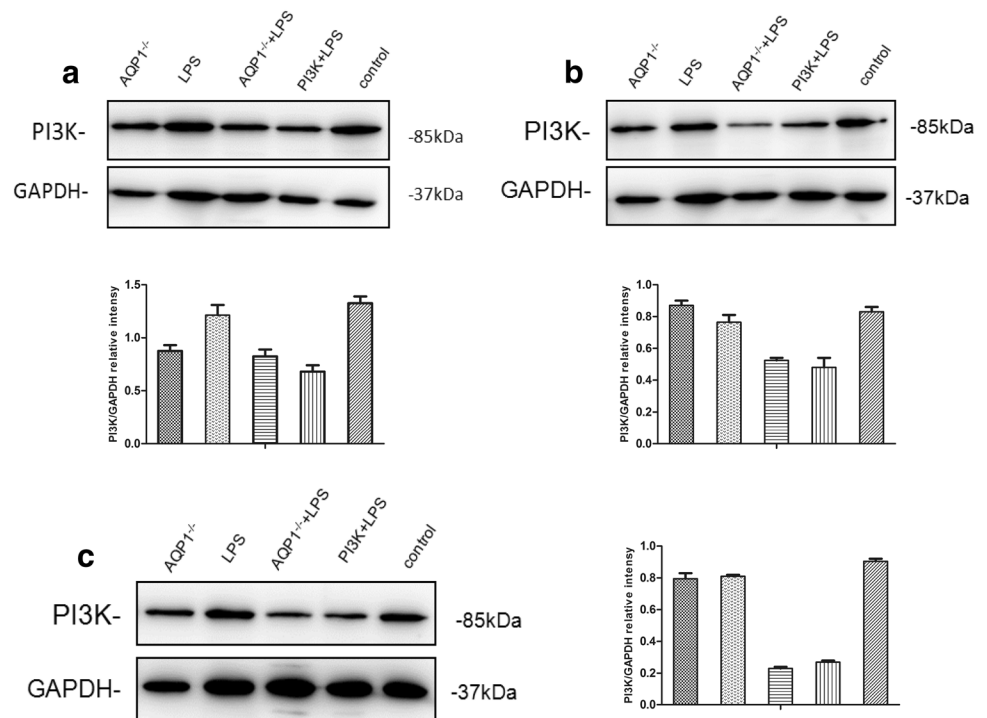


**Fig. 7** Expression of PI3K protein in RAW264.7 cells was determined by western blotting. **a** After 4 h, **b** after 24 h and **c** after 48 h. AQP1<sup>-/-</sup> group: *AQP1* gene silencing group with 100 nM si-AQP1 for 4 h; LPS group: RAW264.7 cells treated with 0.1 μg/mL LPS for 24 h; PI3K + LPS group: cells pretreated with 100 nM PI3K inhibitor (wortmannin) for 1 h and subsequently treated with 0.1 μg/mL LPS for 24 h. 4 h, 24 h and 48 h: time after the withdrawal of LPS



### PI3K inhibition suppressed M2 polarization and increased release of inflammatory factors in LPS-induced RAW264.7

It has been reported that polarization of macrophages is meticulously regulated by intracellular signaling pathways [23]. PI3K is an important intracellular signaling pathway and its role in macrophage polarization has gradually attracted the attention of many researchers. To examine the effect of PI3K on M2 polarization in LPS-induced RAW264.7 cells, we treated cells with the PI3K inhibitor, wortmannin, and compared the levels of M2 polarization markers (CD206 and Arg-1). The formation of cell pseudopodia was observed under an inverted microscope. The ELISA results showed that wortmannin markedly reduced Arg-1 protein levels and decreased the proportion of elongated pseudopodocytes (Fig. 8a–d). Finally, the immunofluorescence staining of CD206 indicated that wortmannin inhibited the translocation of CD206 from the nucleus to the cytoplasm. Taken together, these results showed that inhibition of PI3K decreased M2 polarization.

Next, we examined the expression levels of the inflammatory factors, IL-6, TNF- $\alpha$ , NF- $\kappa$ B and of iNOS. Our ELISA results revealed that the PI3K inhibitor significantly increased the levels of IL-6, TNF- $\alpha$  and iNOS. Immunofluorescence showed that NF- $\kappa$ B activation and translocated to nucleus after treatment with PI3K inhibitor. These results suggest that PI3K inhibitor aggravated inflammation in LPS-induced RAW264.7 cells.

## Discussion

Several risk factors of AKI have been identified, including trauma, severe infection and chronic kidney disease. AKI is the most common complication and major cause of death in patients with sepsis [25]. LPS is one of the effective components of Gram-negative bacteria. It has been reported that LPS treatment promotes the development of AKI [26]. Consistently, our study showed that LPS promoted AKI in

Wistar rats, as indicated by the elevation of serum creatinine and urea nitrogen, renal tubular epithelial cell swelling and inflammatory exudation. The ELISA results also revealed that the expression of the inflammatory factors, TNF- $\alpha$ , IL-6 and iNOS increased in AKI. These results suggest that inflammation is involved in the pathogenesis of AKI induced by sepsis. Zhang et al. have also demonstrated increased release of inflammation factors during renal ischemia–reperfusion injury [27].

AKI is a complex inflammatory disease, in which mainly three cell types are involved, including macrophages in the tissue, exuding inflammatory cells and endothelial cells [1]. The pathophysiological mechanisms by which LPS promotes organ damage, particularly kidney injury, is manifold and complex. Polarization transition of macrophages can regulate the balance between anti-inflammatory and pro-inflammatory factors in the process of inflammation [28]. Additionally, macrophage activation is the initial stage of inflammation and it plays a key role in cascade amplification of inflammation. A previous study has reported that M2 macrophage deficiency aggravates LPS-induced tissue damage and inflammation, implying the importance of M2 macrophages in LPS-induced AKI [29]. Another study has demonstrated that M2 macrophages promote angiogenesis and proliferation of tumor cells [30]. Consistently, our study showed increased expression of M1 markers (iNOS, TNF- $\alpha$ , IL-6) in the early injury stage and increased expression of M2 macrophage markers (Arg-1, CD206) in the late stage of tissue repair.

Our previous study has found that AQP1 protein in the serum and urine was increased in LPS-induced AKI [14]. Hiroko et al. have shown that the expression of *AQP1* mRNA in the renal tissue decreased in ischemia/reperfusion-induced AKI [31]. To explore the role of AQP1 in AKI, renal tissue *AQP1* mRNA and protein were examined. Consistent with a previous study [31], *AQP1* mRNA expression was low during the whole process, while AQP1 protein was increased in the early phase (12 and 24 h) and decreased in the late stage (48 and 72 h). A possible explanation is the compensatory retention mechanism of the organism, that is, the body protects itself against organ damage by reducing the excretion of

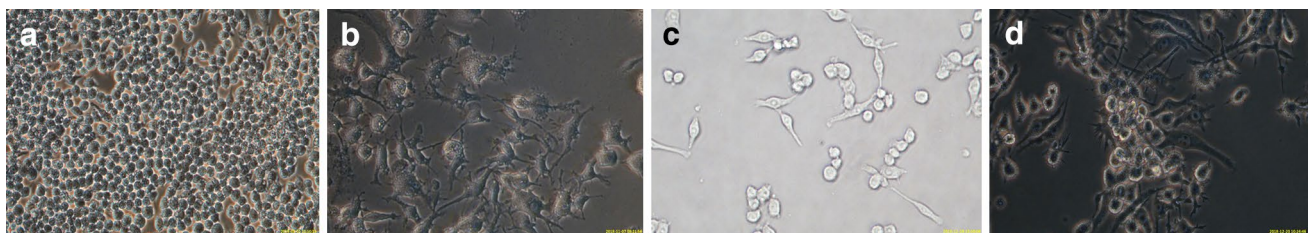


**Fig. 8** Macrophage (RAW264.7 cells) shape of different polarization subtypes. **a** M0 are regular round in shape and without pseudopods. **b** M1 are irregular in shape and with multiple short pseudopods. **c** M2

are regular oval in shape with elongated pseudopods. **d** M0, M1 and M2 coexist (400 $\times$ )

AQP1. Previous studies have also shown that AQP1 reduced LPS-induced HK-2 cell damage and inflammatory response [15]. Another explanation is that AQP1 protein has a long half-life, so when transcription and translation decrease, its protein level does not immediately decline. Another possibility is that when renal tubular epithelial cells are damaged and lysed, AQP1 protein is released into the blood and urine, as previous studies have confirmed that AQP1 is highly expressed in renal tubular epithelial cells.

In our experiment, we found that AQP1 alleviated inflammatory reaction by inducing macrophage M2 polarization in LPS-induced AKI rats. Studies have increasingly found that AQP1 as a water channel play an important role in migration of inflammatory cells, pseudopodium formation and secretion of inflammatory factors [32], therefore, the role of AQP1 in the LPS-induced AKI is multifaceted, because LPS-induced AKI is an inflammatory disease and AQP1 participates in almost all processes of inflammation. Kishore et al. [33] also found that AQP1 plays a key role in cisplatin-induced polyuria AKI, their results showed that renal AQP1 was decreased after intraperitoneal injection of cisplatin in rats. Decreased AQP1 levels led to impaired water reabsorption, which further leads to disordered urine concentration and increased urine volume. Asvapromtada et al. [34] found that there was a positive correlation between the degree of renal injury and the degree of AQP1 decrease in I/R AKI rats (establishment of ischemia–reperfusion AKI by clamping bilateral renal pedicle). What role does AQP1 play in I/R AKI? According to recent research, AQP1 can transport not only water but also CO<sub>2</sub>, O<sub>2</sub> and other gases. Early studies have found that AQP1 has CO<sub>2</sub> permeability [35]. Echevarría et al. [36] proved that AQP1 could facilitate O<sub>2</sub> diffusion across the cell membrane along the concentration gradient, when renal tissue is ischemic and anoxic, intracellular oxygen concentration is higher than that of extracellular, AQP1 can transport O<sub>2</sub> from intracellular to extracellular, therefore, it can reduce the production of intracellular reactive oxygen species (ROS) and reduce mitochondria injury to protect cells and tissue from damage. To summarize, AQP1 plays a role in AKI rats caused by various causes, because the damage mechanism of each AKI is different and AQP1 works in different ways, so a growing number of studies have found that AQP1 is a molecule with complex functions that participate in pathological process of AKI, thus AQP1 is expected to be the target of AKI treatment.

Inflammation involves the exudation of fluids and the release of inflammatory factors. AQP1 as a transport protein is presumed to play an important role in the process of inflammation. Hiroko et al. have found that AQP1 protein is elevated in rats with AKI [31]. Previous studies have also found that AQP5 expression is downregulated in a rat acute lung injury model [37]. Our previous study has also demonstrated that AQP1 overexpression reduced the secretion

of inflammatory factors and cell apoptosis in HK-2 cells [15]. Cell damage and inflammation activation are fundamental characteristics in the initiation and development of AKI. Macrophage polarization as a form of inflammation activation has been confirmed in almost all inflammatory diseases [22] and the transformation between proinflammatory and anti-inflammatory phenotypes determines the prognosis of inflammation. Based on this information, we explored the role of AQP1 in LPS-induced macrophage M2 polarization. A previous research found that AQP1 inhibited M2 polarization of resting macrophages and promoted M2 polarization after LPS stimulation [13]. In contrast to previous experiments, we examined AQP1 protein at different stages of inflammation. Our results showed that AQP1 protein was increased in the early phase (12 and 24 h) and was decreased in the late stage of inflammation (48 and 72 h). In vitro, we found that silencing AQP1 inhibited the expression of M2 markers (CD206 and Arg-1) and increased the secretion of inflammatory factors (IL-6, TNF- $\alpha$  and iNOS) in LPS-induced RAW264.7 cells. Consistently, a previous research found that AQP1 inhibited M2 polarization of resting macrophages and promoted M2 polarization after LPS stimulation [13], indicating that the effect of AQP1 on macrophage polarization depends on the macrophage state. Thus, we speculated that AQP1-induced M2 polarization may be the cellular mechanism by which AQP1 prevents the development of AKI.

Unlike inflammatory cell activation, macrophage polarization requires fine regulation of intracellular signaling pathways. PI3K has been explored in many autophagy experiments. Recent studies have found that PI3K also plays a key role in the initiation and prognosis of inflammation [13]. However, there is little research on this aspect. Upon activation, PI3K induces the synthesis of anti-inflammatory and growth-promoting cytokines (TGF- $\beta$  and IL-10) [38]. In vivo, we found herein that the expression of PI3K was upregulated in rat renal tissue induced by LPS as well as the expression of AQP1. In vitro, silencing AQP1 with siRNA led to a decrease in PI3K and in M2 macrophage markers (CD206 and Arg-1), suggesting that AQP1 promotes PI3K activation and M2 polarization. To study the relationship between PI3K and M2 polarization, we inhibited PI3K in LPS-induced RAW264.7 cells with wortmannin. M2 macrophage markers (CD206 and Arg-1) were suppressed, whereas IL-6, TNF- $\alpha$  and iNOS were increased, suggesting that PI3K is involved in M2 macrophage polarization and inflammation reduction.

Previously, we have revealed that AQP1 protein was increased in LPS-induced Wistar rats, but *AQP1* mRNA was decreased, indicating that the elevation of AQP1 is a protective effect. Overexpression of AQP1 confirmed that AQP1 can indeed reduce the release of inflammatory factors and cell apoptosis in LPS-induced HK-2 cells. To

explore the molecular and cellular mechanisms by which AQP1 alleviates AKI, we carried out this study. In vivo, intraperitoneal injection of LPS into Wistar rats increased renal PI3K expression, elevated renal and serum inflammatory factors (IL-6, iNOS and TNF- $\alpha$ ), increased serum creatinine and urea nitrogen, aggravated renal tissue damage, decreased *AQP1* mRNA and increased AQP1 protein in the early stage and decreased AQP1 protein in the late stage of AKI. Unlike most experiments, we examined the macrophage phenotype at different stages of inflammation to elucidate the phenotypic transformation of macrophages (from proinflammation M1 to anti-inflammation M2). *AQP1* mRNA and AQP1 protein were both detected until 72 h, therefore, we were able to observe the decrease in AQP1 protein in the late stage of inflammation. In vitro, AQP1 silencing or PI3K inhibition increased the LPS-induced inflammatory response by elevating inflammatory cytokines' (IL-6, iNOS, TNF- $\alpha$  and NF- $\kappa$ B) secretion and inhibiting M2 polarization. AQP1 silencing also decreased PI3K expression. In this study, we found that AQP1 not only alleviated inflammation, but it also promoted M2 polarization of macrophages by activating PI3K. Unexpectedly, we also found that AQP1 induces M2 polarization when handling with LPS, however, AQP1 inhibits macrophage M2 polarization when macrophages are quiescent. Our results confirmed the relationship among AQP1, PI3K and macrophage M2 polarization only in vitro, because the organism has a complex regulatory system, as the physiological and pathological changes are regulated by multiple signaling pathways simultaneously. Herein, we only studied one of these pathways. Macrophage polarization is also influenced by the phase of disease; the M1 phenotype is dominant in the early stage of injury and the M2 phenotype gradually increases in the late stage of repair. M2 macrophages play different roles in different diseases, for instance, it has been shown that in allergic diseases caused by parasites, M2 macrophages promote inflammation and aggravate injury [39], whereas M2 macrophages have been shown to play a role in promoting tumor growth [40], therefore, the relationship between AQP1 and M2 polarization still needs to be confirmed by further in vivo experiments.

In conclusion, our results provide evidence that AQP1 alleviated AKI induced by sepsis primarily by its ability to activate PI3K, ultimately resulting in M2 polarization of macrophages. Hence, macrophage M2 polarization is likely a cellular mechanism underlying the protective role of AQP1 in AKI with PI3K activation as the downstream mediator. Targeting PI3K-dependent macrophage M2 polarization, therefore, may be considered a new therapeutic strategy for alleviating AKI caused by sepsis.

**Acknowledgements** We thank Michal Bell, Ph.D., from Liwen Bianji, Edanz Editing China ([www.liwenbianji.cn/ac](http://www.liwenbianji.cn/ac)), for editing the English text of a draft of this manuscript.

**Author contributions** CL and BL performed the experiments. XD, LX, GS and KT analyzed the data. YJ made substantial contributions to conception and design, acquisition of data, analysis and interpretation of data, acquisition of funding. All authors gave their final approval of the version to be published.

**Funding** This study was supported by the Natural Youth Science Foundation of China (grant no. 81501825) and Youth Science Foundation of Heilongjiang Province of China Grant (grant no. QC2012C035).

## Compliance with ethical standards

**Conflict of interest** The authors have no conflict of interest to disclose.

**Ethics statement** The study protocol was approved by the Animal Care and Use Committee of Harbin Medical University (No: 2019014), and the experimental procedures were in accordance with the recommendations of the Guide for the care and use of Laboratory Animals, published by the US National Institutes of Health (NIH Publication no. 85-23. Revised 196).

## References

1. Cohen J. The immunopathogenesis of sepsis. *Nature*. 2002;420:885–91.
2. Li C, Wu J, Li Y, Xing G. Cytoprotective effect of heat shock protein 27 against Lipopolysaccharide-induced apoptosis of renal epithelial HK-2 cell. *Cell Physiol Biochem*. 2017;41:2211–20.
3. Rivers EP, Coba V, Whitmill M. Early goal-directed in severe sepsis and septic shock: a contemporary review of the literature. *Curr Opin Anaesthesiol*. 2008;21:128–40.
4. Zhong F, Chen H, Han L, Jin Y, Wang W. Curcumin attenuates lipopolysaccharide-induced renal inflammation. *Biol Pharm Bull*. 2011;34:226–32.
5. Monzani E, Bazzotti R, Perego C, La Porta CA. AQP1 is not only a water channel: it contributes to cell migration through Lin7/ beta-catenin. *PLoS ONE*. 2009;4:e6167.
6. Stock C, Schwab A. Ion channels and transporters in metastasis. *Biochim Biophys Acta*. 2015;1848:2638–46.
7. Pelagalli A, Nardelli A, Fontanella R, et al. Inhibition of AQP1 hampers osteosarcoma and hepatocellular carcinoma progression mediated by bone marrow-derived mesenchymal stem cells. *Int J Mol Sci*. 2016;17(7):1102.
8. Jin Y, Yu G, Peng P, Zhang Y, Xin X. Down-regulated expression of AQP5 on lung in rat DIC model induced by LPS and its effect on the development of pulmonary edema. *Pulm Pharmacol Ther*. 2013;26:661–5.
9. Jiang YX, Dai ZL, Zhang XP, Zhao W, Huang Q, Gao LK. Dexmedetomidine alleviates pulmonary edema by upregulating AQP1 and AQP5 expression in rats with acute lung injury induced by lipopolysaccharide. *Huazhong Univ Sci Technol Med Sci*. 2015;35:684–8.
10. Nielsen S, Kwon TH, Frokiaer J, Agre P. Regulation and dysregulation of aquaporins in water balance disorders. *Intern Med*. 2007;261:53–64.
11. Marrone J, Danielli M, Gaspari CI, Marinelli RA. Adenovirus-mediated human aquaporin-1 expression in hepatocytes

- improves lipopolysaccharide-induced cholestasis. *IUBMB Life*. 2017;69:978–84.
12. Li J, Zhang M, Mao Y, Li Y, Zhang X, Peng X, Yu F. The potential role of aquaporin1 on aristolochic acid I induced epithelial mesenchymal transition on HK-2 cells. *Cell Physiol*. 2018;233:4919–25.
  13. Tyteca D, Nishino T, Debaix H, Van Der Smissen P, N'kuli F, Hoffmann D, et al. Regulation of macrophage motility by the water channel aquaporin-1: crucial role of M0/M2 phenotype switch. *PLoS ONE*. 2015;10(2):e0117398.
  14. Dong XY, Liu CM, Li BH, et al. Correlation between urinary aquaporin level and inflammatory factors in disseminated intravascular coagulation with acute non-oliguric renal injury. *Chin J Pract Diagn Treat*. 2019;33(3):216–20.
  15. Wang YD, Zhang WZ, Yu GZ, Liu Q, Jin YY. Cytoprotective effect of aquaporin1 against lipopolysaccharide-induced apoptosis and inflammation of renal epithelial HK-2 cells. *Exp Ther Med*. 2018;15:4243–52.
  16. Langenberg C, Wan L, Egi M, May CN, Bellomo R. Renal blood flow in experimental septic acute renal failure. *Kidney Int*. 2006;69:1996–2002.
  17. Martinez FO. Regulators of macrophage activation. *Eur J Immunol*. 2011;41(6):1531–4.
  18. Martinez FO, Sica A, Mantovani A, et al. Macrophage activation and polarization. *Front Biosci*. 2008;13:453.
  19. Sun K, He SB, Qu JG, et al. IRF5 regulates lung macrophages M2 polarization during severe acute pancreatitis in vitro. *World J Gastroenterol*. 2016;22(42):9368–77.
  20. Watanabe T, Kudo M, Strober W. Immunopathogenesis of pancreatitis. *Mucosal Immunol*. 2017;10(2):283–98.
  21. Humphreys BD. Targeting endogenous repair pathways after AKI. *J Am Soc Nephrol*. 2016;27:990–7.
  22. Huen SC, Cantley LG. Macrophages in renal injury and repair. *Annu Rev Physiol*. 2017;79:449–69.
  23. Zhou Y, Tu C, Zhao Y, et al. Placental growth factor enhances angiogenesis in human intestinal microvascular endothelial cells via PI3K/Akt pathway: potential implications of inflammation bowel disease. *Biochem Biophys Res Commun*. 2016;470(4):967–74.
  24. Burke JE, Williams RL. Synergy in activating class PI3Ks. *Trends Biochem Sci*. 2015;40(2):88–100.
  25. Zarjou A, Agarwal A. Sepsis and acute kidney injury. *J Am Soc Nephrol JASN*. 2011;22:999–1006.
  26. Doi K, Leelahavanichkul A, Yuen PS, Star RA. Animal models of sepsis and sepsis-induced kidney injury. *J Clin Investig*. 2009;119:2868–78.
  27. Zhang Y, Chen J, Zhang K, et al. Inflammation and oxidative stress are associated with the prevalence of high ankle-brachial index in metabolic syndrome patients without chronic renal failure. *Int J Med Sci*. 2013;10(2):183–90.
  28. Qin H, Holdbrooks AT, Liu Y, et al. SOCS3 deficiency promotes M1 macrophage polarization and inflammation. *J Immunol*. 2012;189:3439–48.
  29. Liu X, Mu GH, Song C, Zhou L, et al. Role of M2 macrophages in sepsis-induced acute kidney injury. *Shock*. 2018;50(2):233–9.
  30. Noy R, Pollard JW. Tumor-associated macrophages: from mechanisms to therapy. *Immunity*. 2014;41(1):49–61.
  31. Sonoda H, Yokota-Ikeda N, Oshikawa S, Kanno Y. Decreased abundance of urinary exosomal aquaporin-1 in renal ischemia-reperfusion injury. *Am J Physiol Renal Physiol*. 2009;297:F1006–F10161016.
  32. Tyteca D, Nishino T, Debaix H, et al. Regulation of macrophage motility by the water channel aquaporin-1: crucial role of M0/M2 phenotype switch. *PLoS ONE*. 2015;10(2):e0117398.
  33. Kishore BK, Krane CM, Di Iulio D, et al. Expression of renal aquaporins 1, 2, and 3 in a rat model of cisplatin-induced polyuria. *Int Soc Nephrol*. 2000;58:701–11.
  34. Asvapromtada S, Sonoda H, Kinouchi M, et al. Characterization of urinary exosomal release of aquaporin-1 and -2 after renal ischemia-reperfusion in rats. *Am J Physiol Renal Physiol*. 2018;314:F584–F601.
  35. Nakhoul NL, Davis BA, Romero MF, Boron WF. Effect of expressing the water channel aquaporin-1 on the CO<sub>2</sub> permeability of *Xenopus* oocytes. *Am J Physiol*. 1998;274:C543–8.
  36. Echevarría M, Muñoz-Cabello AM, Sánchez-Silva R, et al. Development of cytosolic hypoxia and hypoxia-inducible factor stabilization are facilitated by aquaporin-1 expression. *J Biol Chem*. 2007;282(41):30207–155.
  37. Jiao G, Li E, Yu R. Decreased expression of AQP1 and AQP5 in acute injured lungs in rats. *Chin Med J (Engl)*. 2002;15:963–7.
  38. Biswas SK, Mantovani A. Macrophage plasticity and interaction with lymphocyte subsets: cancer as a paradigm. *Nat Immunol*. 2010;11(10):889–96.
  39. Dasgupta P, Keegan AD. Contribution of alternatively activated macrophages to allergic lung inflammation: a tale of mice and men. *Innate Immun*. 2012;4:478–88.
  40. Hao NB, Lu MH, Fan YH, Cao YL, Zhang ZR, et al. Macrophages in tumor microenvironments and the progression of tumors. *Clin Dev Immunol*. 2012;9:480–98.

**Publisher's Note** Springer Nature remains neutral with regard to jurisdictional claims in published maps and institutional affiliations.